Alternative splicing and the intracellular domain mediate TM-agrin's ability to differentially regulate the density of excitatory and inhibitory synapse-like specializations in developing CNS neurons

Gerry Handara[1,2,] and Stephan Kröger[1*]

[1]Department of Physiological Genomics, Biomedical Center, Ludwig-Maximilians-University, Großhaderner Str. 9, D-82152 Planegg-Martinsried, Germany

[2] Institute for Stem Cell Research, German Research Center for Environmental Health, Helmholtz Centre Munich, Ingolstädter Landstraße 1, D-85764 Neuherberg, Germany

*To whom correspondence should be addressed:

Stephan Kröger, Department of Physiological Genomics, Biomedical Center, Ludwig-Maximilians-University, Großhaderner Str. 9, D-82152 Planegg-Martinsried, Germany

Email: skroeger@lmu.de

phone +49-89-2180-71899

Fax: +49 89 2180 75216

Running title: Mapping of TM-agrin-induced synaptic changes

Abbreviations:

AChR	acetylcholine receptor
Lrp4	low-density lipoprotein receptor-related protein 4
TM-agrin	transmembrane agrin
NMJ	neuromuscular junction
CNS	central nervous system
MuSK	muscle specific kinase
vGAT	vesicular GABA transporter
GFP	green fluorescent protein
PSD-95	post synaptic density protein 95 kDa
DIV	days *in vitro*
VGluT1	vesicular glutamate transporter 1
$GABA_A$ receptor	γ-aminobutyrate receptor A
mEPSC	miniature excitatory post synaptic current

ABSTRACT

Agrin is a multi-domain protein best known for its essential function during formation of the neuromuscular junction. Alternative mRNA splicing at sites named y and z in the C-terminal part of agrin regulates its interaction with a receptor complex consisting of the agrin-binding protein Lrp4 and the tyrosine kinase MuSK. Isoforms with inserts at both splice sites bind to Lrp4, activate MuSK and are synaptogenic at the neuromuscular junction. Agrin is also expressed as a transmembrane protein in the CNS but its function during interneuronal synapse formation is unclear. Recently we demonstrated that transfection of a full-length cDNA coding for TM-agrin in cultured embryonic cortical neurons induced an Lrp4-dependent but MuSK-independent increase in dendritic glutamatergic synapses and an Lrp4- and MuSK-independent reduction of inhibitory synapses. Here we show that presynaptic specializations were similarly affected by TM-agrin overexpression. In addition, we mapped the regions within TM-agrin responsible for TM-agrin‘s effects on dendritic aggregates synapse-associated proteins. We show that the presence of a four amino acid insert at splice site y is essential for the increase in PSD-95 puncta. This effect was independent of splice site z. The reduction of the gephyrin puncta density was independent of the entire extracellular part of TM-agrin but required a highly conserved serine residue in the intracellular domain of TM-agrin. These results provide further evidence for a function of TM-agrin during CNS synaptogenesis and demonstrate that different domains and alternative splicing of TM-agrin differentially affect excitatory and inhibitory synapse formation in cultured embryonic CNS neurons.

Key words: synaptogenesis, agrin, vGAT, vGluT1, PSD-95, $GABA_A$ receptor, collybistin, gephyrin

INTRODUCTION

Agrin is a heparansulfate proteoglycan that is widely expressed in many tissues, including the central nervous system (CNS; Kröger et al., 2009; Tintignac et al., 2015). Agrin's function is best characterized at the neuromuscular junction (NMJ), where it binds to a receptor complex consisting of the low-density lipoprotein receptor-related protein 4 (Lrp4) and the muscle-specific tyrosine kinase MuSK (Kim et al., 2008; Zhang et al., 2008; Wu et al., 2010). Binding of agrin to Lrp4 activates MuSK and initiates an intracellular signaling cascade that leads to the formation of most, if not all postsynaptic specializations, including aggregates containing the acetylcholine receptor (AChR) and other molecules (Tintignac et al., 2015; Wu et al., 2010; Li et al., 2018). The formation of these specializations is required for synaptic transmission and, accordingly, mice without agrin, Lrp4 or MuSK never form functional NMJs and die perinatally due to non-functional respiratory musculature (Gautam et al., 1996; DeChiara et al., 1996; Weatherbee et al., 2006).

Agrin has been cloned from several species and in all vertebrates, the agrin cDNA predicts a number of structural domains with similarity to other extracellular matrix proteins (see Fig. 1A). In particular, the C-terminal LG3 domain of agrin is necessary and sufficient for Lrp4 binding and synaptogenesis at the NMJ (Gesemann et al., 1995; Kim et al., 2008). The functions of the other domains are mostly unknown (Burgess et al., 2002).

The primary transcript of the *AGRN* gene is subject to alternative mRNA splicing and splicing regulates agrin's synaptogenic activity at the NMJ (Ruegg et al., 1992). In the C-terminal part of agrin, alternative splicing occurs at two sites called "y" and "z" in mammals and "A" and "B" in chicken, respectively. Alternative splicing at splice site z within the LG3 domain generates multiple agrin isoforms that differ in their biological activity (Ruegg et al., 1992; Burgess et al., 1999). Only isoforms with an insert of 8, 11 or 19 amino acid at splice site z are able to bind to Lrp4, activate MuSK and induce postsynaptic specializations at the NMJ (Kim et al., 2008; Zhang et al., 2008; Zong et al., 2012). The functions of agrin isoforms without an insert at the z splice site are unknown.

Distinct transcriptional start sites and alternative first exon usage generate two N-terminal agrin isoforms. Secreted soluble agrin (NtA-agrin) contains an N-terminal NtA domain which stably anchors agrin to basal laminae (Kammerer et al., 1999; Mascarenhas et al., 2003). Alternatively, the NtA domain can be replaced by a non-cleaved signal anchor. This converts agrin into a type II transmembrane protein with a 28 amino acid (mouse) intracellular domain (TM-agrin; Burgess et al., 2000; Neumann et al., 2001). Transcripts coding for TM-agrin isoforms are enriched in embryonic CNS neurons particularly during active axonal elongation and synaptogenesis (Burgess et al., 2000), whereas glial cells in the CNS express only NtA-agrin. The functions of the intracellular domain of TM-agrin and the role of alternative splicing of TM-agrin in developing CNS neurons are unknown.

We have recently shown that transfection of full-length murine TM-agrin cDNA into cultured embryonic cortical neurons resulted in an Lrp4-dependent increase in dendritic PSD-95- and NMDA receptor NR1-subunit-containing synapses and an Lrp4- and MuSK-independent decrease of gephyrin-

and $GABA_A$ receptor α1-subunit-containing synapses (Handara et al., 2019). In the present study, we identify the structural prerequisites for this effect. Specifically, we investigated if alternative splicing regulates agrin's function during formation of interneuronal synapses and if the same domain within TM-agrin affects excitatory and inhibitory synapse-like specializations. We show that alternative splicing at TM-agrin's y- but not z splice site regulates the density of excitatory synapse-like structures. In contrast, a highly conserved serine residue in the cytoplasmic part of TM-agrin is required for the reduction of the density of puncta containing inhibitory synapse-associated proteins. Thus, different domains within TM-agrin affect the formation and/or maintenance of excitatory and inhibitory synapse-like specializations. In addition, our study provides the first evidence for a function of alternative splicing and of the intracellular part of TM-agrin during synaptogenesis of embryonic CNS neurons.

EXPERIMENTAL PROCEDURES

Mice

Use and care of animals was approved by German authorities and according to national law (TierSchG§7). The animal procedures were performed according to the guidelines from directive 2010/63/EU of the European Parliament on the protection of animals used for scientific purposes. All experiments were approved by the local authorities of the State of Bavaria, Germany (Az.: ROB-55.2-2532.Vet_02-17-82). C57BL/6J wild-type mice were bred in the animal facility of the Biomedical Center of the Ludwig-Maximilians-University Munich. Animals were housed on a 12/12 h light/dark cycle with free access to food and water. The day of the vaginal plug was considered embryonic day 0.5 (E 0.5). Forty-five embryos derived from 14 pregnant mice were used in this study. Embryonic cortical neurons were prepared from 36 embryos from 11 mice and immunocytochemical analysis was performed on 9 additional embryos from 3 different mice.

Monolayer cultures

Monolayer cultures from embryonic mouse cortices were prepared by trypsinization and trituration with fire-polished Pasteur pipettes as described (Hilgenberg et al., 2007; Sciarretta et al., 2010) with the modifications detailed in Hartfuss et al. (2001), Walcher et al. (2013) and Handara et al. (2019). In brief, 18 mm coverslips were treated overnight with sodium hydroxide/ethanol, subsequently incubated with 1M hydrochloric acid and then stored in absolute ethanol. Coverslips were coated with poly-D-lysine (0.01 mg/ml in PBS) overnight under sterile conditions, washed with sterile water and then sterilized by dry heat. Cells from embryonic day 14.5 mice were seeded at a density of 100.000 cells per well in 12-well plates (growth area 3.8 cm^2/well) and cultivated for 14 days *in vitro* (DIV) in 1 ml neurobasal medium (Invitrogen) supplemented with B27 supplement, GlutaMAX and penicillin-streptomycin (Thermo Fisher Scientific, Munich, Germany).

Cloning and assembly of mouse transmembrane agrin cDNA

The cDNA coding for the N-terminal transmembrane and for the C-terminal domains were obtained from a C57BL/6 embryonic mouse head cDNA library, using the polymerase chain reaction. The remaining sequence coding for the middle segment of TM-agrin was obtain by restriction digest (SfiI and ApaLI; New England Biolabs, Frankfurt, Germany) from the commercially available pCR- XL- TOPO-BC150703.1- Agrin clone (Imagene Source Bioscience, Notthingham, UK). The mouse full-length cDNA was assembled from these fragments by homologous recombination using the yeast strain CAY29 (MATa ura3-52; Andreasson et al., 2002). The cDNA was then purified from yeast and the full-length TM-agrin cDNA inserted into the bicistronic pMES vector (Swartz et al., 2001). This vector contains an internal ribosomal entry site regulating the simultaneous expression of the gene of interest together with the enhanced green fluorescent protein (GFP). This allowed the convenient distinction of the few transfected from the majority of untransfected cells (Karakatsani et al., 2017; Handara et al., 2019). The GFP signal was routinely intensified by staining with anti-GFP antibodies.

Transfection

Transfection of cortical neurons with Lipofectamine 2000 (Invitrogen, Karlsruhe, Germany) was performed on DIV 12 according to the manufacturer's instructions with the modifications described by Masserdotti et al., 2015, Shi et al., 2018 and Karakatsani et al., 2017. In brief, embryonic cortical neurons in each well were transfected with 500 ng of plasmid DNA and 0.5 µl Lipofectamine in a total volume of 100 µl of neurobasal medium per well. Transfection of a pMES vector without a cDNA insert (pMES-GFP) was used as control. The number of transfected cells was in the range of 2% and the transfection efficiency was independent of the cDNA insert.

The following full-length mouse TM-agrin cDNAs were used (Fig. 1): TM-agriny4z8, TM-agriny0z0 and TM-agriny4z0 (Fig.1). The deletion constructs (TM-agrin FD8, TM-agrin FD6, TM-agrin ΔEC, Fig.1) were generated as previously described (Porten et al., 2010). The constructs containing point mutations (TM-agrinS17A, TM-agrinS17D) were generated commercially by site-directed mutagenesis (Genscript Biotech Corporation, Piscataway, NJ, USA). All constructs were routinely sequenced to detect mutations and subject to diagnostic restriction digest. No attempt was made to quantify the expression levels of the different TM-agrin constructs in neurons, but HEK cells transfected with the different constructs, expressed approximately similar levels. Some of the deletion constructs have previously been shown to code for proteins that are normally posttranslational processed and trafficked to the membrane (Porten et al., 2010).

Antibodies and immunocytochemistry

After 14 days *in vitro*, neuronal cultures were fixed in 4% paraformaldehyde in PBS for 10 minutes at room temperature followed by washing, blocking and permeabilization with 2% bovine serum albumin and 0.2% Triton X-100 in PBS (Zhang et al., 2015; Karakatsani et al., 2017). The following antibodies were used: anti-PSD-95 (mouse monoclonal IgG2a, clone 7E3-1B8, Thermo Fisher Scientific); anti-VGluT1 (polyclonal guinea pig antiserum, Cat. No. 135 304, Synaptic Systems, Göttingen, Germany); anti-gephyrin (rabbit polyclonal, Cat. No. 147 002; Synaptic Systems); anti-$GABA_A$ receptor α1-subunit (rabbit polyclonal, Cat. No. 06-868, Merck, Darmstadt, Germany); anti-$GABA_A$ receptor α5-subunit (rabbit polyclonal, Cat. No. 224503, Synaptic Systems); anti-collybistin (rabbit polyclonal, Cat. No. 261003, Synaptic Systems); anti-vGAT (guinea pig polyclonal, Cat. No. 131004, Synaptic Systems), anti-GFP (chicken polyclonal, Cat. No. ab13970, Abcam), anti-Tbr1 (mouse monoclonal Santa Cruz, Cat. No. sc-376258; rabbit polyclonal Cat. No. ab31940, Abcam) and anti-NMDA receptor NR1-subunit (mouse monoclonal, Merck, Cat. No. Mab363). As secondary antibodies, we used highly pre-absorbed, Alexa Fluor-conjugated antibodies directed against the appropriate species and monoclonal isotype (Alexa-488, Alexa-594 and Alexa-647; Thermo Fisher Scientific).

Quantitative analysis of synaptic puncta in embryonic cortex cultures

Images of single neurons for quantification of excitatory (vGluT1 and PSD-95) and for inhibitory (vGAT, collybistin, gephyrin) synapse-associated proteins were acquired using an Axio ImagerM2 epifluorescence microscope equipped with a C-Apochromat 40x, NA 1.2 water immersion objective and the ZEN 2010 software (Carl Zeiss GmbH, Jena, Germany). The soma of a neuron was placed in the center of the image and a zoom factor of one was chosen.

Puncta of excitatory- and inhibitory synapse-associated proteins were counted unbiased as described previously (Handara et al., 2019). In brief, cultures were stained with the appropriate antibodies. The number of pixels above the threshold was then automatically determined using the Particle Analysis tool of the Fiji platform (Schindelin et al., 2012) by employing the protocol previously described (Ippolito et al., 2010). To this end individual images were transformed into 'binary' black and white images by converting the corresponding channel into 8-bit format. A threshold value was then applied to differentiate between object of interest and background using the global automatic thresholding function. This thresholding was optimized so that the representative binary image best matched the synaptic puncta of the source images. The same threshold value was then used for the control and for the experimental images, respectively. A region of interest on the dendrite (20 µm x 5 µm) was selected and pixels within a distance of <1µm of the GFP-filled dendrite were scored to avoid a contribution of neighboring neurons and their processes. The results were expressed as puncta per 20 µm of dendrite and puncta were defined automatically as aggregates of pixels above threshold with a diameter between 0.1 and 1 µm.

Since excitatory and inhibitory synapses are not evenly distributed along the dendrite, the number of puncta per 20 μm associated with excitatory synapses was determined on distal dendrites outside a radius of 50 μm from the soma (Klenowski et al., 2015). In contrast, punctate immunoreactivity with antibodies against inhibitory synapse-associated proteins was determined on dendrites within a radius of 50 μm from the soma (Klenowski et al., 2015). Transfected neurons but not transfected glial cells were randomly selected and the analysis was performed double-blind. Dendritic segments overlapping with highly stained somata and puncta that were not unambiguously associated with the dendrite of a transfected cell were not included in the analysis.

Statistical analysis

Results are presented as the median with interquartile range in a dot plot. One randomly chosen neuron per well was used in the analysis as one experimental unit, i.e. a dot represents a neurons in which at least three randomly chosen dendritic segments were analyzed and averaged. Neurons from 3 different pregnant mice dissected at three different time points were investigated. Significance was calculated with GraphPad Prism vs.8 (GraphPad Software, San Diego, California) using the Mann-Whitney U test or the Kruskal-Wallis-test with Dunn's posthoc correction for multiple comparisons. The type 1 statistical error was set to 5% ($\alpha = 0.05$). The level of significance (P-value) for all statistical tests was set at *P<0.05, **P<0.01, ***P<0.001.

RESULTS

<u>Transfection of embryonic CNS neurons with TM-agrin cDNA induces an increase in presynaptic specializations at excitatory synapses</u>

We recently demonstrated that transfection of the TM-agrin isoform y4z8 (TM-agriny4z8, see Fig. 1A,B) into embryonic cortical neurons induced an increase in the density of dendritic puncta containing PSD-95 or the NR1 subunit of the NMDA receptor. Moreover, addition of soluble agrin to individual embryonic cortical neurons resulted in an increase in miniature excitatory postsynaptic current (mEPSC) frequency and amplitude (Handara et al., 2019). These results suggested an increase in the density of dendritic excitatory synapses in response to agrin. To extend these results, we investigated if other C-terminal splice variants had a similar effect and if presynaptic glutamatergic specializations were similarly affected. To this end, we transfected embryonic cortical neurons with TM-agriny4z0 cDNA, stained them with antibodies against PSD-95 or against the vesicular glutamate transporter 1 (vGluT1) and analyzed the density of these puncta. We observed an increase in the density of PSD-95 puncta on the dendrites of neurons transfected with TM-agriny4z0 that was comparable to the increase observed after transfection of TM-agriny4z8 (Fig. 2A-C). Moreover, the density of vGluT1 puncta in close apposition to dendrites of neurons transfected with the TM-agriny4z0 construct was similarly increased compared to the dendrites of neurons transfected with the

pMES-GFP control vector (Fig. 2 D-F). Thus, the increase in the density of postsynaptic excitatory synapse-like specializations was accompanied by a corresponding increase in the density of presynaptic specializations.

Alternative splicing at the y site regulates TM-agrin's ability to increase the density of excitatory synapse-associated proteins

To investigate, if alternative splicing regulates the increase of PSD-95 puncta density, we transfected cultured embryonic cortical neurons with different TM-agrin C-terminal splice variants (see Fig. 1A,B for the different TM-agrin isoforms). Transfection of these neurons with a full-length cDNA coding for the TM-agrin isoform y4z0 (TM-agriny4z0, Fig. 1B), which is synthesized by neurons but has negligible AChR aggregation activity at the NMJ (Ruegg et al., 1992; Ferns et al., 1992; Ferns et al., 1993; Gesemann et al., 1995), increased the density of dendritic PSD-95 puncta (Fig. 3A,D). A similar increase was observed in neurons transfected with a cDNA coding for TM-agriny4z8 (Fig. 3B,D), which is expressed by neurons, binds to Lrp4 and has AChR aggregation activity (Gesemann et al., 1995; Burgess et al., 2000; Neumann et al., 2001; Zong et al., 2012). Thus, the increase in dendritic PSD-95 puncta density was independent of the z splice site and, thus, did not require a direct high-affinity binding to Lrp4. In contrast, transfection with a cDNA coding for the TM-agriny0z0 isoform did not increase the density of PSD-95 puncta (Fig. 3C,D), or the density of puncta labeled with antibodies against vGluT1 and the NR1 subunit of the NMDA receptor (data not shown). This demonstrates that the presence of a 4 amino acid insert at the y splice site is required for the TM-agrin-mediated increase in the density of pre- and postsynaptic excitatory synapse-associated proteins.

Transfection of embryonic CNS neurons with TM-agrin cDNA induces a decrease in the density of inhibitory synapse-associated proteins but has no influence on non-synaptic inhibitory neurotransmitter receptors

Previously we reported a decrease in the density of dendritic puncta containing the inhibitory synapse-associated proteins gephyrin and the α1-subunit of the $GABA_A$ receptor in response to transfection with cDNA coding for TM-agriny4z8 (Handara et al., 2019). To investigate if other inhibitory synapse-associated proteins were similarly affected, we stained neurons transfected either with the control vector or with full-length mouse TM-agriny4z0 cDNA using antibodies against the gephyrin-associated GDP/GTP exchange factor collybistin (Kins et al., 2000). We observed a decrease in the density of dendritic collybistin puncta in neurons transfected with the TM-agriny4z0 cDNA compared to neurons transfected with the pMES-GFP vector (Fig. 4 A-C). This demonstrates that z-TM-agrin isoforms have a similar effect on inhibitory synapses as z+ isoforms. Moreover, our results show that other proteins aggregated postsynaptically at inhibitory synapses are similarly affected by TM-agrin overexpression.

To investigate if presynaptic specializations of inhibitory synapses are similarly reduced, we stained transfected neurons with antibodies against the vesicular GABA transporter (vGAT). We observed a decrease in vGAT puncta density in presynapse-like structures terminating on neurons transfected with TM-agriny4z0 (Fig. 4 D-F) compared to presynapses on neurons transfected with the pMES-GFP vector. This demonstrates that the TM-agrin overexpression-mediated reduction of inhibitory postsynaptic specializations is accompanied by a reduction of the corresponding presynaptic specializations.

We next analyzed the distribution of the $GABA_A$ receptor α5-subunit ($GABA_A$R-α5), which is predominantly localized on dendrites outside of inhibitory CNS synapses (Brickley et al., 2012; Brady et al., 2015). Transfection of TM-agriny4z0 cDNA did not apparently affect the distribution and the density of dendritic puncta of the $GABA_A$R-α5 subunit (Fig. 4 G-I). These results show that, while transfection with TM-agrin cDNA decreased the density of puncta containing the synaptic α1-subunit (Handara et al., 2019), gephyrin or collybistin, it did not decrease the mostly non-synaptic α5-subunit containing $GABA_A$ receptor puncta.

Increase of excitatory and decrease of inhibitory synapses occurs in the same Tbr1-positive neuron

To investigate if the TM-agrin-induced reduction of inhibitory- and increase in excitatory synapse-like specializations occurred in separate populations of neurons, we investigated both types of synapses in Tbr1-positive neurons. Tbr1-positive neurons represent glutamatergic cortical pyramidal neurons, which receive excitatory and inhibitory input (Kolk et al., 2006). We observed no difference in the density of Tbr1-positive neurons in cultures transfected with the pMES-GFP control vector or with the pMES vector containing TM-agrin cDNA (data not shown), demonstrating that there is no selective loss of this particular type of neuron due to the transfection. Analysis of the density of puncta on dendrites of Tbr1-positive neurons stained with antibodies against PSD-95 (Fig. 5 A,B,C) or against gephyrin (Fig. 5 D,E,F) revealed that transfection with the TM-agriny4z0 construct increased excitatory and decreased inhibitory synapse-like specializations in Tbr1-positive neurons. This demonstrates that transfection of TM-agrin cDNA affects both excitatory and inhibitory synapses in this specific neuronal population.

To investigate if TM-agrin transfection affects excitatory- and inhibitory synapse-like specializations in the same neuron, individual cortical neurons were transfected with cDNA coding for TM-agriny4z0 and the density of excitatory and inhibitory synapse-associated proteins was determined on dendritic segments of the same neuron. We observed an increase in the number of PSD-95-positive puncta and a decrease of the gephyrin puncta within the same dendrite when neurons transfected with TM-agriny4z0 (Fig. 6 E-H) were compared with neurons transfected with the pMES vector (Fig. 6 A-D). Collectively, these results demonstrate that transfection of TM-agrin alters both types of synapses simultaneously in the same neuron and that the differential effect of TM-agrin

overexpression on excitatory and inhibitory synapse-associated proteins is not due to selective effect on specific subpopulations of neurons.

A conserved serine residue in the intracellular region of TM-agrin is required for the TM-agrin-mediated reduction of the density of inhibitory synapse-like specializations

To investigate which domain of TM-agrin mediates the reduction of the density of puncta containing inhibitory synapse-associated proteins, we transfected several isoforms and deletion constructs into embryonic cortical neurons. Transfection of neurons with constructs lacking parts of the extracellular domain of TM-agrin (see Fig. 1B for a schematic representation of the various deletion constructs), reduced the density of gephyrin puncta to the same extent, as did transfection with full-length TM-agriny4z0 cDNA (Fig. 7 A,B,C). Likewise, removal of the entire extracellular region (TM-agrin ΔEC, Fig. 1 B) did not influence the ability of TM-agrin to reduce gephyrin puncta density (Fig. 7 E). In contrast, the pMES-GFP control vector did not affect the density of dendritic inhibitory synapses (Fig. 7 A,C; Handara et al., 2019). These results demonstrate that the extracellular part of TM-agrin is dispensable, and that the intracellular and/or the transmembrane region of TM-agrin are sufficient to downregulate the density of dendritic gephyrin puncta.

To precisely map the region within the cytoplasmic part of TM-agrin required to reduce the number of inhibitory synapse-associated proteins, we mutated the serine residue at position 17 of the intracellular region to alanine (TM-agrinS17A, see Fig. 1C). This serine was initially chosen since it is highly conserved between species. Transfection of the TM-agrinS17A cDNA into cortical neurons did not reduce dendritic gephyrin puncta density (Fig. 7 D,F), demonstrating that the presence of this serine residue is required for the TM-agrin-mediated decrease in the density of inhibitory synapse-associated proteins.

The serine 17 residue represents a consensus sequence for phosphorylation. Since the mutation from serine to alanine is predicted to be non-phosphorylatable, we wanted to investigate the effect of a phosphomimetic mutation. To this end, we substituted serine by aspartic acid (TM-agrinS17D). This mutation is predicted to mimic a permanently phosphorylated serine. Remarkably, transfection of the phosphomimetic TM-agrinS17D mutant cDNA reduced the density of dendritic gephyrin puncta similar to wildtype full-length TM-agrin cDNA (Fig. 7 E,F). In contrast, the density of excitatory synapse-like specializations was not affected by any of the serine 17 mutations (data not shown). Collectively, our results demonstrate that the extracellular domain of TM-agrin is dispensable for the TM-agrin-mediated decrease of inhibitory synapse-like specializations. Instead, the conserved intracellular serine17 residue appears essential. These results also demonstrate that the TM-agrin-

mediated increase in excitatory- and the decrease in inhibitory synapse-like specializations are independent of each other and are mediated by different regions within the TM-agrin protein.

DISCUSSION

Little is known about the role of agrin during formation of synapses in the developing CNS. Analysis of the cortex from adult agrin-deficient brains revealed a decrease in pre- and postsynaptic specializations at excitatory synapses and a decrease in the frequency of mEPSCs, but no changes at inhibitory synapses (Ksiazek et al., 2007), suggesting a role for agrin during formation or maintenance of excitatory synapses *in vivo*. We showed previously that TM-agrin overexpression in embryonic cortical neurons resulted in an Lrp4-dependent increase in the number of dendritic excitatory synapses and a decrease in the density of inhibitory synapses (Handara et al., 2019). In the present study, we provide evidence that the effects of TM-agrin on excitatory and inhibitory synapse-like specializations are mediated by distinct regions within the TM-agrin protein and that presynaptic specializations are similarly affected.

At the NMJ, only agrin isoforms that contain a peptide insert of 8, 11 or 19 amino acids at splice site z are synaptogenic through their direct high-affinity binding to Lrp4 (Ruegg et al., 1992; Hoch et al., 1993; Gesemann et al., 1996; Zong et al., 2012). Likewise, TM-agriny4z8 is able to induce AChR aggregates in cultured myotubes (Neumann et al., 2001), suggesting that the appropriate TM-agrin isoform can also interact with Lrp4. Interestingly, we show that TM-agriny4z0 and TM-agriny4z8 isoforms similarly increased the number of dendritic excitatory synapse-like structures, suggesting that alternative mRNA splicing at splice site z did not apparently regulate TM-agrin's function at developing synapses in the CNS. Although we cannot rule out an additional low-affinity binding site common to both TM-agrin isoforms, our results suggest that a direct interaction of the TM-agrin LG3 domain with Lrp4 was not required to elicit this effect in cultured embryonic CNS neurons. On the other hand, the increase of dendritic excitatory synapse-like specializations was not observed in Lrp4-deficient neurons (Handara et al., 2019), suggesting that Lrp4 expression is required for the TM-agrin-medicated effect on excitatory synapse-like specialization. Collectively, we interpret the results that an indirect interaction of TM-agrin and Lrp4 is required for the TM-agrin-induced increase in dendritic PSD-95 puncta density.

We identified serine at position 17 of TM-agrin as essential for the reduction of the density of inhibitory synapse-associated proteins, including gephyrin, collybistin and the $GABA_AR$ α1-subunit. This serine was initially chosen because it is highly conserved between species and because it is the only amino acid within the intracellular part of TM-agrin that is predicted to be a consensus sequence for phosphorylation. Phosphorylation is essential for the agrin-dependent AChR aggregation at the NMJ (Wallace et al., 1991) and for gephyrin aggregation at CNS synapses (Tyagarajan et al., 2011; Kuhse et al., 2012; Battaglia et al., 2018). While transfection of the cDNA containing the phosphomimetic serine to aspartic acid mutation reduced the density of inhibitory synapses similar to

wildtype full-length cDNA, transfection of full-length TM-agrinS17A cDNA (a mutation that renders this site non-phosphorylatable) was ineffective. Combined, these findings suggest that serine17 may be phosphorylated and that this phosphorylation regulates TM-agrin's effect on inhibitory synapse-like specializations.

It remains to be determined which kinase phosphorylates TM-agrin at serine 17. Analysis of the intracellular amino acid sequence using the online open-access platform Netphos3.1 (Blom et al., 2004; http://www.cbs.dtu.dk/services/NetPhos) revealed that the only kinase predicted to be able to phosphorylate TM-agrin at serine 17 is the CDK1 kinase. CDK1 is a member of the cyclin-dependent kinase family, which promote the transitions between the different cell cycle phases (Morgan, 1997). CDK1 (encoded by the *cdc2* gene) has been localized to the cytoplasm during G1/S/G2 phase and enters the nucleus after the breakdown of the nuclear lamina (Bailly et al., 1989). Interestingly, CDK1 has previously been shown to phosphorylate gephyrin and this phosphorylation regulates gephyrin clustering in the postsynaptic membrane at inhibitory synapses (Kuhse et al., 2012). It will be interesting to investigate if TM-agrin and gephyrin might both be substrates of the same serine kinase. In any case, more detailed experiments are required to directly demonstrate the phosphorylation of serine17 and the potential function of CDK1 in regulating TM-agrin activity.

Interestingly, overexpression of TM-agrin reduced the number of clusters containing gephyrin, collybistin or the α1 subunit of the $GABA_A$ receptor but did not affect the distribution of the $GABA_AR$ α5 subunit. The α5 subunit assembles with β and γ subunits, is primarily localized extrasynaptically (Brunig et al., 2002; Christie et al., 2002; Brickley et al., 2012), and is mainly responsible for generating tonic inhibition in the hippocampal pyramidal neurons (Glykys et al., 2008). However, the α5 subunit is also able to directly bind to gephyrin and some of these $GABA_A$ receptor complexes can be detected at inhibitory synapses (Brady et al., 2015). It remains to be determined if TM-agrin can influence the gephyrin-associated synaptic α5 subunit pool. In cultured embryonic cortical neurons, however, this was apparently not the case. Instead, TM-agrin primarily affected the distribution of the synapse-associated α1 $GABA_A$ receptor subunit, demonstrating a specificity of the TM-agrin activity towards synaptically aggregated proteins.

Transfection of TM-agrin cDNA into CNS neurons has previously been shown to induce the formation of filopodia-like processes (Porten et al., 2010; Ramseger et al., 2009; McCroskery et al., 2006; McCroskery et al., 2009). Since filopodia can function as precursors for dendritic spines (Berry et al., 2017), it was hypothesized that TM-agrin might influence glutamatergic synapse formation by increasing the number of these filopodia-like protrusions (Kröger et al., 2009; Daniels, 2012). In the present study, we show that splice site y regulates the formation of excitatory synapse-like specializations. In contrast, filopodia-like process formation was independent of the intracellular and the C-terminal half of TM-agrin but instead required an aspartic acid residue within the 7th follistatin-like domain (Porten et al., 2010). Thus, the increase of excitatory synapse-like specializations and the formation of filopodia-like processes involved different regions within the TM-agrin protein,

suggesting that these processes are independent of each other. Thus, the function of the TM-agrin-induced filopodia-like processes in the developing CNS remains to be determined but they are unlikely to contribute to the aggregation of excitatory synapse-associated proteins.

Agrin-deficient mice whose perinatal death was rescued by re-expressing agrin selectively in motoneurons using the HB9 promotor ("rescue mice") have a reduced number of and functional deficits in excitatory synapses complementary to the increase of excitatory synapses observed in TM-agrin overexpressing neurons (Ksiazek et al., 2007; Handara et al., 2019). In contrast, the density of inhibitory synapses were affected in TM-agrin overexpressing neurons (Handara et al., 2019), but not in the rescue mice (Ksiazek et al., 2007). Our mapping of the site responsible for the effect on inhibitory synapses to serine 17 in the intracellular domain of TM-agrin might provide an explanation for this discrepancy: In the agrin-deficient mouse line, used to generate the rescue mice, a PGK-Neo cassette was inserted downstream of exon 6 of the *AGRN* gene (Lin et al., 2001). This replaced most of agrin's coding region (including the region required for AChR aggregation at the NMJ) but left the first five exons intact. These exons contain the intracellular as well as the transmembrane region of TM-agrin and, thus, this fragment might still be expressed. We show that the expression of the intracellular and transmembrane region is sufficient to maintain the integrity of inhibitory synapses *in vitro* and hypothesize that it might also be sufficient *in vivo*. Due to the expression of the N-terminal fragment of TM-agrin, inhibitory synapses might not be affected in the rescue mice. Along the same line, the identification of serine 17 as an essential residue regulating the density of dendritic inhibitory synapse-like specializations might explain why the addition of soluble agrin (lacking the intracellular and the transmembrane domain) to microisland cultures from embryonic cortical neurons had no effect on the electrophysiological properties of inhibitory synapses (Handara et al., 2019).

In summary, our study maps two specific effects of TM-agrin overexpression in embryonic CNS neurons to distinct regions within the TM-agrin protein: Splicing at the y-site regulates TM-agrin's activity at excitatory synapse-like specializations, and serine 17 in the intracellular domain appears to be required for the reduction of inhibitory synapses. In addition to assigning particular functions to specific regions within the TM-agrin protein, our results further support a role for TM-agrin during synapse formation in the developing CNS and adds to the growing body of evidence that formation of the NMJ shares molecular determinants with synaptogenesis in the developing CNS.

ACKNOWLEDGEMENTS

We thank I. Vitali for expert technical assistance. We are grateful to John Bixby, Fritz Rathjen, Hansruedi Brenner and Giovanna Sonsalla for critical reading and improving of the manuscript and Magdalena Götz for constant support and encouragement.

DECLRATION OF INTEREST

None

FUNDING

This research did not receive any specific grant from funding agencies in the public, commercial, or not-for-profit sectors.

Figure captions

Figure 1: Schematic representation of the domain structure predicted by the agrin cDNA and of the constructs used to identify the regions responsible for the effect of TM-agrin on excitatory and inhibitory synapses. Panel A shows the domain structure of agrin, including the splice sites "y" and "z" in the C-terminal half of agrin. Alternative first exon usage results in the synthesis of either a soluble, basal lamina-associated agrin (NtA-agrin) or of an isoform in which the NtA domain is replaced by a single membrane-spanning region and a short intracellular sequence (TM-agrin). The various structural domains within the agrin protein are specified underneath the full-length agrin protein. Panel B shows the different C-terminal splice variants and the deletion constructs used in this study. Panel C illustrates the amino acid sequence of the intracellular region with the single amino acid substitutions (shown in red letters within the green rectangle) used to determine the region required for the TM-agrin-mediated reduction of the density of inhibitory synapse-like specializations.

Figure 2: Transfection of embryonic neurons with TM-agriny4z0 increases presynaptic vGluT and postsynaptic PSD-95 puncta density. Embryonic cortical neurons were transfected with either the control pMES vector coding for GFP (pMES-GFP; green channel; A,D) or with the same vector containing the TM-agrin y4z0 cDNA (B,E) and stained with antibodies against PSD-95 (red channel in panels A,B) or against the vesicular glutamate transporter (vGluT1; red channel in D,E). The insets in panels A, B, D and E show higher magnifications of the boxed regions to illustrate the density of PSD-95 and vGluT puncta, respectively, on the dendrites of transfected neurons. The outline of the dendrites are shown by white lines in the insets. Selected individual puncta scored in the quantification were marked with a circle in the insets. Note that neurons transfected with TM-agrin cDNA have a higher density of PSD-95 ($U_{10,9} = 14$) and vGluT1 puncta ($U_{7,7} = 6$) on their dendrites. Quantification is shown in panels C and F, respectively, in a scatter dot plot (median with interquartile range). Each dot represents the mean of at least 3 dendritic segments of the same neuron. Scale bar in E: 50µm.

Figure 3: A four amino acid insert at splice site y is required for the TM-agrin-mediated increase in PSD-95 puncta. Embryonic cortical neurons were transfected with either a TM-agrin isoform which interacts with Lrp4 and is active in AChR aggregation at the neuromuscular junction (TM-agriny4z8; B) or with isoforms that do not interact with Lrp4 and have no AChR aggregation activity (TM-agrin y4z0; A; or TM-agriny0z0; C). The green channel shows the GFP fluorescence of the transfected neurons. The red channel shows the PSD-95 staining. The insets show the boxed areas at higher magnification. The dendrite is outlined by white lines. PSD-95 puncta density was determined on dendrites outside a 50 µm radius around the cell body (indicated by the white circles in panels A-C). Quantification of the dendritic PSD-95 density after transfection of the various constructs is shown in

panel D as a dot plot (median with interquartile range). Only cDNAs encoding a four amino acid insert at splice site y increased the density of dendritic PSD-95 puncta. Statistical significance was determined using the Kruskal-Wallis test ($H(3)=31.89$; $p<0.001$) with Dunn's correction for multiple comparisons. Scale bar in C: 50µm.

Figure 4: Transfection with TM-agriny4z0 cDNA decreases the density of dendritic collybistin and vGAT puncta but does not affect the density of puncta containing the $GABA_A$ receptor α5-subunit. Embryonic cortical neurons were transfected with the pMES vector coding for GFP (pMES-GFP; green channel in panels A,D,G) or with the same vector coding additionally for TM-agriny4z0 (green channel in panels B, E, H). Neurons were stained with antibodies against collybistin (red channel in A,B), the vesicular GABA transporter (vGAT; red channel in D,E) or the α5-subunit of the $GABA_A$ receptor ($GABA_A$R-α5; red channel in G,H). Insets show the boxed areas at higher magnification. White lines in the insets outline the dendrites. The density of inhibitory synapse-associated proteins was determined within a radius of 50 µm around the cell body (white circles). Quantification of the puncta density showed that transfection of neurons with TM-agriny4z0 cDNA reduced the density of collybistin (C; $U_{6,5} = 0$) and vGAT puncta (F; $U_{9,9} = 6.5$) but did not affect the density of puncta stained with antibodies against the α5-subunit of the $GABA_A$ receptor (I; $U_{5,10} = 24.5$). Quantification is shown as a dot plot (median with interquartile range). Each dot represents the mean of at least 3 different dendritic segments of one neuron. Scale bar in A: 50µm.

Figure 5: Excitatory and inhibitory synapses are affected in the same neuron. Cortical pyramidal neurons were identified by staining with anti-Tbr1 antibodies. Tbr1-positive neurons (purple channel) transfected with the TM-agriny4z0 cDNA were were compared to neurons transfected with the pMES vector. The density of puncta stained with anti-PSD-95 (A,B,E) or anti-gephyrin antibodies (C,D,F), respectively, in segments of 20 µm length of dendrites of transfected neurons was then determined. Quantifications are shown as dot plots (median with interquartile range) with each dot representing the mean of at least 3 dendritic segments of one neuron. Quantification revealed that in this particular neuronal subpopulation, transfection with TM-agrin caused an increase in excitatory synapse-like specializations and a decrease in inhibitory synapse-like specializations ($U_{5,6} = 0$) that was similar to the change observed previously when all transfected neurons were analyzed. Scale bar in A: 50 µm

Figure 6: Transfection of TM-agriny4z0 increase the density of PSD-95 puncta and decreases the density of gephyrin puncta in dendrites of the same neuron. Embryonic cortical neurons transfected with either the empty pMES vector (pMES-GFP; A-D) or with TM-agriny4z0 (E-H) were stained simultaneously with antibodies against gephyrin (A,E) and against PSD-95 (B,F). The boxed areas

represent higher magnifications shown in the insets in panels A,B,E,F). The position of the boxes with respect to the dendrites of the transfected neurons are indicated in panels C and G. Quantifications are shown as dot plots (median with interquartile range) with each dot representing the mean of at least 3 dendritic segments of one neuron. Determination of the number of PSD-95 (D) and gephyrin (H) puncta in dendritic segments of 20 µm length on the same transfected neurons revealed an increase in the number of PSD-95 puncta (D; $U_{5,5} = 0$) and a decrease of gephyrin puncta (H; $U_{5,5} = 0$), demonstrating that TM-agrin overexpression simultaneously affected both types of synaptic specializations in the same neuron. Scale bar in C and G: 10 µm

Figure 7: The serine 17 residue is required for the TM-agrin-mediated reduction of inhibitory synapse-associated protein puncta density. Transfected embryonic cortical neurons (green fluorescence in panels A,B,D,E) were stained with antibodies against gephyrin (red channel in A,B,D,E). Transfection with the empty pMES vector (pMES-GFP in A,C,F) did not affect gephyrin puncta density, whereas transfection with full-length TM-agriny4z0 cDNA (B,C,F) significantly reduced dendritic gephyrin puncta density. These results were quantified by determining the number of gephyrin puncta / 20 µm segment of dendrite (C,F). The density of gephyrin puncta was similarly reduced by all constructs having mutations in the extracellular domain (C; see Fig. 1B for the structure of the different constructs). In contrast, transfection with a full-length TM-agrin cDNA in which serine17 was mutated to alanine (TM-agrinS17A) did not reduce gephyrin puncta density (D,F). Transfection of the phosphomimetic mutation of serine17 to aspartic acid cDNA (TM-agrinS17D) reduced gephyrin puncta density to the same extent as did the transfection of full-length wildtype TM-agrin cDNA (E,F). Due to the large number of neurons analyzed (given in parenthesis above or below the data points), only a single dot representing the median and interquartile range is shown. Statistical significance was determined using the Kruskal-Wallis test with Dunn's correction for multiple comparisons (panel C; $H(6) = 38.81$, $p<0.001$; panel F; $H(3) = 25.68$, $p<0.001$). Scale bar in A: 50 µm

References

Andreasson C, Ljungdahl PO (2002), Receptor-mediated endoproteolytic activation of two transcription factors in yeast. Genes Dev 16:3158-3172.

Bailly E, Doree M, Nurse P, Bornens M (1989), p34cdc2 is located in both nucleus and cytoplasm; part is centrosomally associated at G2/M and enters vesicles at anaphase. EMBO J 8:3985-3995.

Battaglia S, Renner M, Russeau M, Come E, Tyagarajan SK, Levi S (2018), Activity-Dependent Inhibitory Synapse Scaling Is Determined by Gephyrin Phosphorylation and Subsequent Regulation of GABAA Receptor Diffusion. eNeuro 5:doi: 10.1523/ENEURO.

Blom N, Sicheritz-Ponten T, Gupta R, Gammeltoft S, Brunak S (2004), Prediction of post-translational glycosylation and phosphorylation of proteins from the amino acid sequence. Proteomics 4:1633-1649.

Brady ML, Jacob TC (2015), Synaptic localization of alpha5 GABA (A) receptors via gephyrin interaction regulates dendritic outgrowth and spine maturation. Dev Neurobiol 75:1241-1251.

Brickley SG, Mody I (2012), Extrasynaptic GABA(A) receptors: their function in the CNS and implications for disease. Neuron 73:23-34.

Brunig I, Scotti E, Sidler C, Fritschy JM (2002), Intact sorting, targeting, and clustering of gamma-aminobutyric acid A receptor subtypes in hippocampal neurons in vitro. J Com Neurol 443:43-55.

Burgess RW, Nguyen QT, Son YJ, Lichtman JW, Sanes JR (1999), Alternatively spliced isoforms of nerve- and muscle-derived agrin: Their roles at the neuromuscular junction. Neuron 23:33-44.

Burgess RW, Skarnes WC, Sanes JR (2000), Agrin isoforms with distinct amino termini: Differential expression, localization, and function. J Cell Biol 151:41-52.

Christie SB, de Blas AL (2002), alpha5 Subunit-containing GABA(A) receptors form clusters at GABAergic synapses in hippocampal cultures. Neuroreport 13:2355-2358.

Daniels MP (2012), The role of agrin in synaptic development, plasticity and signaling in the central nervous system. Neurochem Int 61:848-853.

DeChiara TM, Bowen DC, Valenzuela DM, Simmons MV, Poueymirou WT, Thomas S, Kinetz E, Compton DL, et al. (1996), The receptor tyrosine kinase MuSK is required for neuromuscular junction formation in vivo. Cell 85:501-512.

Ferns M, Hoch W, Campanelli JT, Rupp F, Hall ZW, Scheller RH (1992), RNA splicing regulates agrin-mediated acetylcholine receptor clustering activity on cultured myotubes. Neuron 8:1079-1086.

Ferns MJ, Campanelli JT, Hoch W, Scheller RH, Hall ZW (1993), The ability of agrin to cluster AChRs depends on alternative splicing and on cell surface proteoglycans. Neuron 11:491-502.

Gautam M, Noakes PG, Moscoso L, Rupp F, Scheller RH, Merlie JP, Sanes JR (1996), Defective neuromuscular synaptogenesis in agrin-deficient mutant mice. Cell 85:525-535.

Gesemann M, Cavalli V, Denzer AJ, Brancaccio A, Schumacher B, Ruegg MA (1996), Alternative splicing of agrin alters its binding to heparin, dystroglycan, and the putative agrin receptor. Neuron 16:755-767.

Gesemann M, Denzer AJ, Ruegg MA (1995), Acetylcholine receptor aggregating activity of agrin isoforms and mapping of the active site. J Cell Biol 128:625-636.

Glykys J, Mann EO, Mody I (2008), Which GABA(A) receptor subunits are necessary for tonic inhibition in the hippocampus? J Neurosci 28:1421-1426.

Handara G, Hetsch FJA, Jüttner R, Schick A, Haupt C, Rathjen FG, Kröger S (2019), The role of agrin, Lrp4 and MuSK during dendritic arborization and synaptogenesis in cultured embryonic CNS neurons. Dev Biol 445:54-67.

Hartfuss E, Galli R, Heins N, Götz M (2001), Characterization of CNS precursor subtypes and radial glia. Dev Biol 229:15-30.

Hilgenberg LG, Smith MA (2007), Preparation of dissociated mouse cortical neuron cultures. J Vis Exp 10:562.

Hoch W, Ferns M, Campanelli JT, Hall ZW, Scheller RH (1993), Developmental regulation of highly active alternatively spliced forms of agrin. Neuron 11:479-490.

Ippolito DM, Eroglu C (2010), Quantifying synapses: an immunocytochemistry-based assay to quantify synapse number. J Vis Exp doi: 10.3791/2270.:2270.

Kammerer RA, Schulthess T, Landwehr R, Schumacher B, Lustig A, Yurchenco PD, Ruegg MA, Engel J, et al. (1999), Interaction of agrin with laminin requires a coiled-coil conformation of the agrin-binding site within the laminin gamma 1 chain. EMBO J 18:6762-6770.

Karakatsani A, Marichal N, Urban S, Kalamakis G, Ghanem A, Schick A, Zhang Y, Conzelmann KK, et al. (2017), Neuronal LRP4 regulates synapse formation in the developing CNS. Development 144:4604-4615.

Kim N, Stiegler AL, Cameron TO, Hallock PT, Gomez AM, Huang JH, Hubbard SR, Dustin ML, et al. (2008), Lrp4 is a receptor for Agrin and forms a complex with MuSK. Cell 135:334-342.

Kins S, Betz H, Kirsch J (2000), Collybistin, a newly identified brain-specific GEF, induces submembrane clustering of gephyrin. Nat Neurosci 3:22-29.

Klenowski PM, Fogarty MJ, Belmer A, Noakes PG, Bellingham MC, Bartlett SE (2015), Structural and functional characterization of dendritic arbors and GABAergic synaptic inputs on interneurons and principal cells in the rat basolateral amygdala. J Neurophysiol 114:942-957.

Kolk SM, Whitman MC, Yun ME, Shete P, Donoghue MJ (2006), A unique subpopulation of Tbr1-expressing deep layer neurons in the developing cerebral cortex. Mol Cell Neurosci 32:200-214.

Kröger S, Pfister H (2009), Agrin in the nervous system - synaptogenesis and beyond. Future Neurol 4:67-86.

Ksiazek I, Burkhardt C, Lin S, Seddik R, Maj M, Bezakova G, Jucker M, Arber S, et al. (2007), Synapse loss in cortex of agrin-deficient mice after genetic rescue of perinatal death. J Neurosci 27:7183-7195.

Kuhse J, Kalbouneh H, Schlicksupp A, Mukusch S, Nawrotzki R, Kirsch J (2012), Phosphorylation of gephyrin in hippocampal neurons by cyclin-dependent kinase CDK5 at Ser-270 is dependent on collybistin. J Biol Chem 287:30952-30966.

Li L, Xiong WC, Mei L (2018), Neuromuscular Junction Formation, Aging, and Disorders. Annu Rev Physiol 80:159-188.

Lin WC, Burgess RW, Dominguez B, Pfaff SL, Sanes JR, Lee KF (2001), Distinct roles of nerve and muscle in postsynaptic differentiation of the neuromuscular synapse. Nature 410:1057-1064.

Mascarenhas JB, Ruegg MA, Winzen U, Halfter W, Engel J, Stetefeld J (2003), Mapping of the laminin-binding site of the N-terminal agrin domain (NtA). EMBO J 22:529-536.

Masserdotti G, Gillotin S, Sutor B, Drechsel D, Irmler M, Jorgensen HF, Sass S, Theis FJ, et al. (2015), Transcriptional Mechanisms of Proneural Factors and REST in Regulating Neuronal Reprogramming of Astrocytes. Cell Stem Cell 17:74-88.

McCroskery S, Bailey A, Lin L, Daniels MP (2009), Transmembrane agrin regulates dendritic filopodia and synapse formation in mature hippocampal neuron cultures. Neuroscience 163:168-179.

McCroskery S, Chaudhry A, Lin L, Daniels MP (2006), Transmembrane agrin regulates filopodia in rat hippocampal neurons in culture. Mol Cell Neurosci 33:15-28.

Morgan DO (1997), Cyclin-dependent kinases: engines, clocks, and microprocessors. Annu Rev Cell Dev Biol 13:261-291.

Neumann FR, Bittcher G, Annies M, Schumacher B, Kröger S, Ruegg MA (2001), An alternative amino-terminus expressed in the central nervous system converts agrin to a type II transmembrane protein. Mol Cell Neurosci 17:208-225.

Porten E, Seliger B, Schneider VA, Wöll S, Stangel D, Ramseger R, Kröger S (2010), The process-inducing activity of transmembrane agrin requires follistatin-like domains. J Biol Chem 285:3114-3125.

Ramseger R, White R, Kröger S (2009), Transmembrane form agrin-induced process formation requires lipid rafts and the activation of Fyn and MAPK. J Biol Chem 284:7697-7705.

Ruegg MA, Tsim KW, Horton SE, Kröger S, Escher G, Gensch EM, McMahan UJ (1992), The agrin gene codes for a family of basal lamina proteins that differ in function and distribution. Neuron 8:691-699.

Schindelin J, Arganda-Carreras I, Frise E, Kaynig V, Longair M, Pietzsch T, Preibisch S, Rueden C, et al. (2012), Fiji: an open-source platform for biological-image analysis. Nature methods 9:676-682.

Sciarretta C, Minichiello L (2010), The preparation of primary cortical neuron cultures and a practical application using immunofluorescent cytochemistry. Methods Mol Biol 633:221-231.

Shi B, Xue M, Wang Y, Wang Y, Li D, Zhao X, Li X (2018), An improved method for increasing the efficiency of gene transfection and transduction. Int J Physiol Pathophysiol Pharmacol 10:95-104.

Swartz M, Eberhart J, Mastick GS, Krull CE (2001), Sparking new frontiers: Using in vivo electroporation for genetic manipulations. Dev Biol 233:13-21.

Tintignac LA, Brenner HR, Ruegg MA (2015), Mechanisms Regulating Neuromuscular Junction Development and Function and Causes of Muscle Wasting. Physiol Rev 95:809-852.

Tyagarajan SK, Ghosh H, Yevenes GE, Nikonenko I, Ebeling C, Schwerdel C, Sidler C, Zeilhofer HU, et al. (2011), Regulation of GABAergic synapse formation and plasticity by GSK3beta-dependent phosphorylation of gephyrin. Proc Natl Acad Sci U S A 108:379-384.

Walcher T, Xie Q, Sun J, Irmler M, Beckers J, Ozturk T, Niessing D, Stoykova A, et al. (2013), Functional dissection of the paired domain of Pax6 reveals molecular mechanisms of coordinating neurogenesis and proliferation. Development 140:1123-1136.

Wallace BG, Qu Z, Huganir RL (1991), Agrin induces phosphorylation of the nicotinic acetylcholine receptor. Neuron 6:869-878.

Weatherbee SD, Anderson KV, Niswander LA (2006), LDL-receptor-related protein 4 is crucial for formation of the neuromuscular junction. Development 133:4993-5000.

Wu H, Xiong WC, Mei L (2010), To build a synapse: signaling pathways in neuromuscular junction assembly. Development 137:1017-1033.

Zhang B, Luo S, Wang Q, Suzuki T, Xiong WC, Mei L (2008), LRP4 serves as a coreceptor of agrin. Neuron 60:285-297.

Zhang Y, Lin S, Karakatsani A, Rüegg MA, Kröger S (2015), Differential regulation of AChR clustering in the polar and equatorial region of murine muscle spindles. Eur J Neurosci 41:69-78.

Zong Y, Zhang B, Gu S, Lee K, Zhou J, Yao G, Figueiredo D, Perry K, et al. (2012), Structural basis of agrin-LRP4-MuSK signaling. Genes Dev 26:247-258.

Figure 1
Click here to download high resolution image

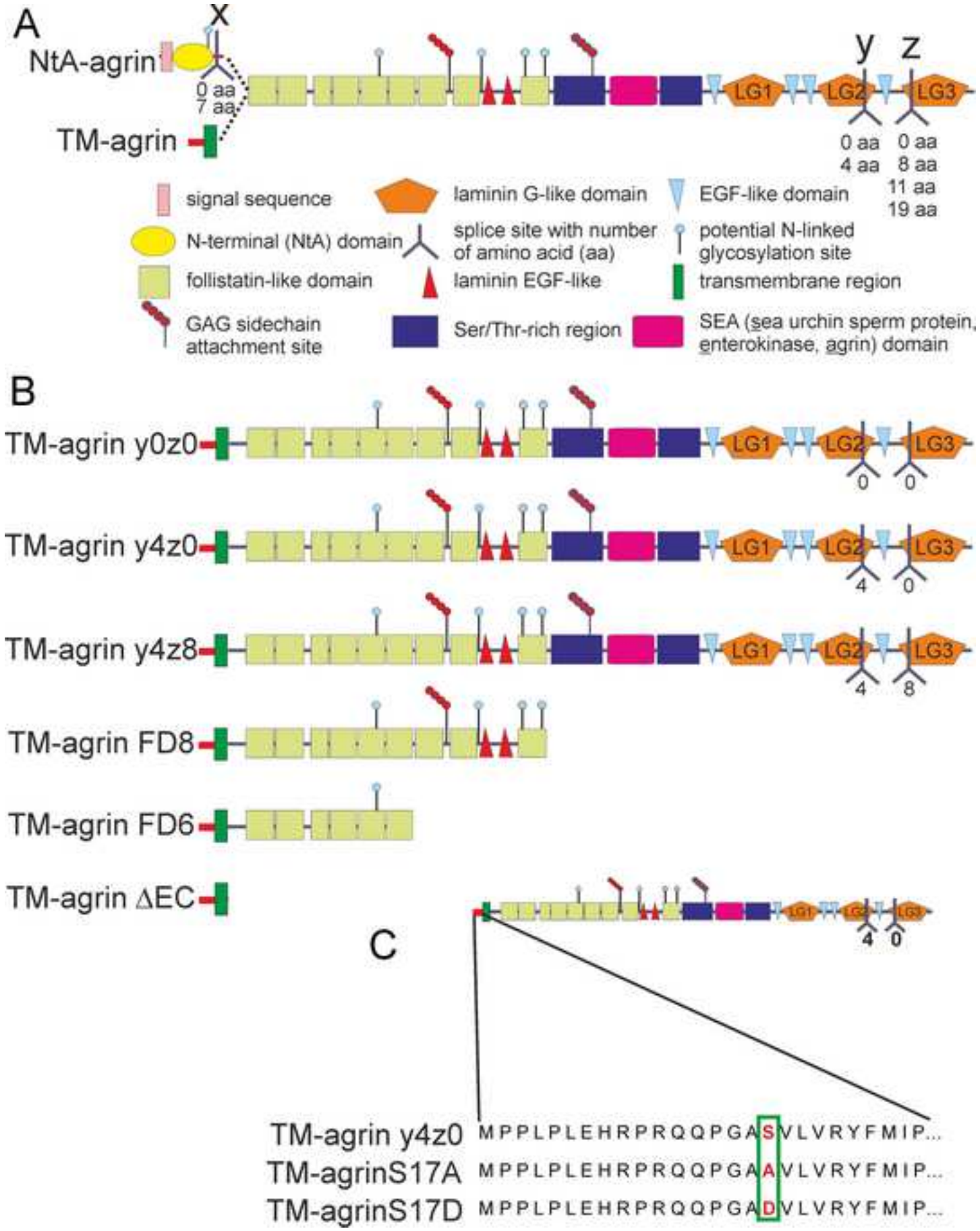

Figure 2

Click here to download high resolution image

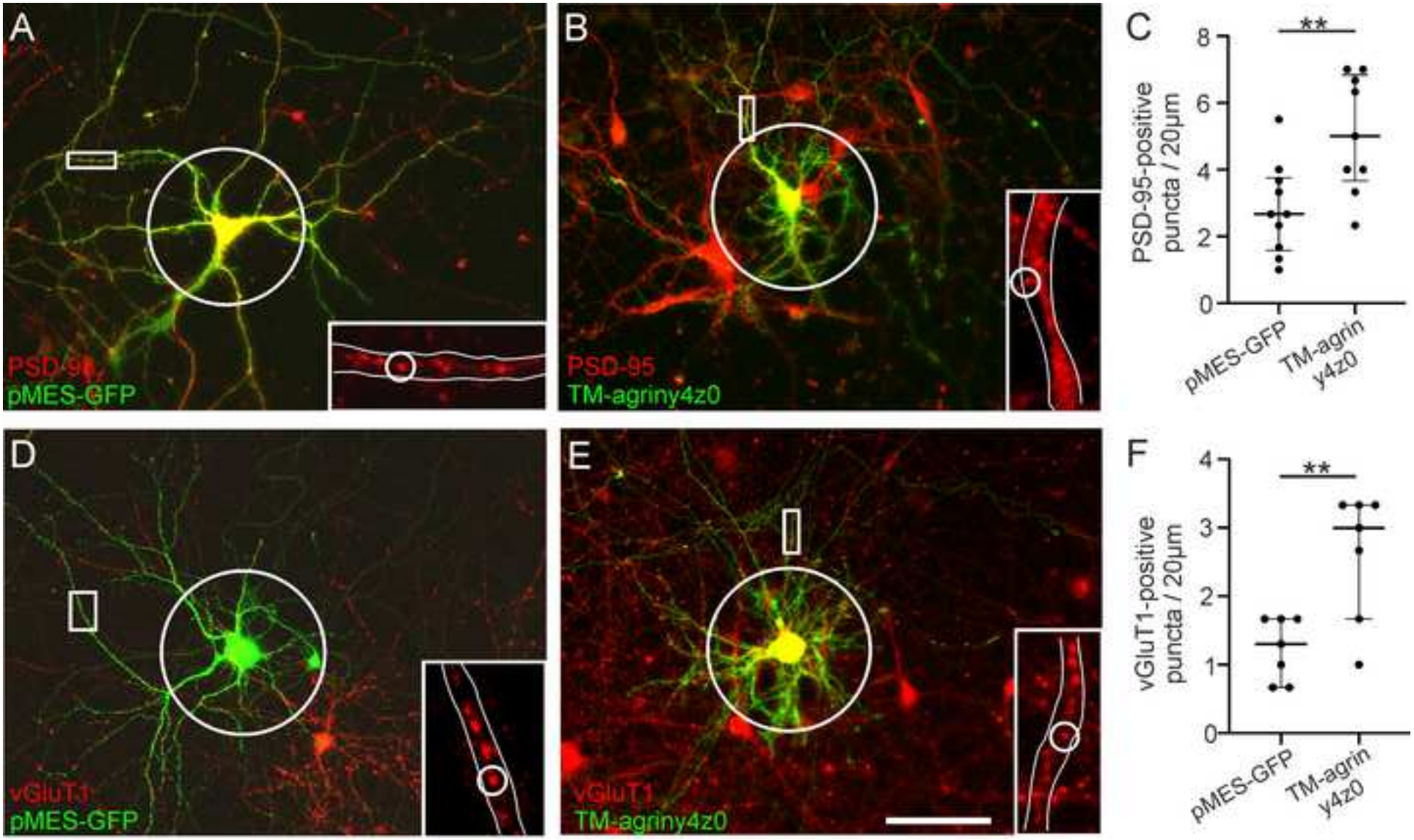

Figure 3

Click here to download high resolution image

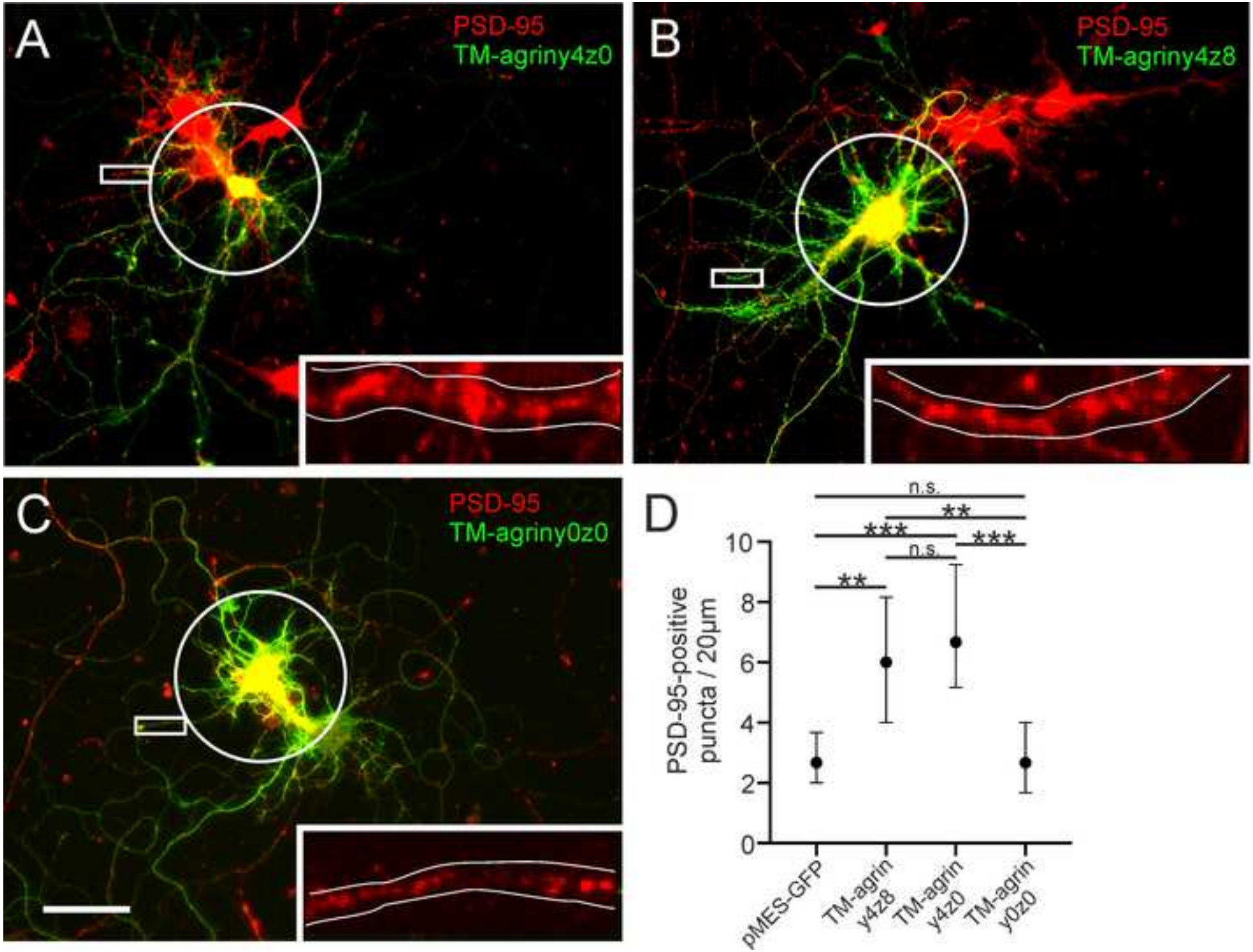

Figure 4

Click here to download high resolution image

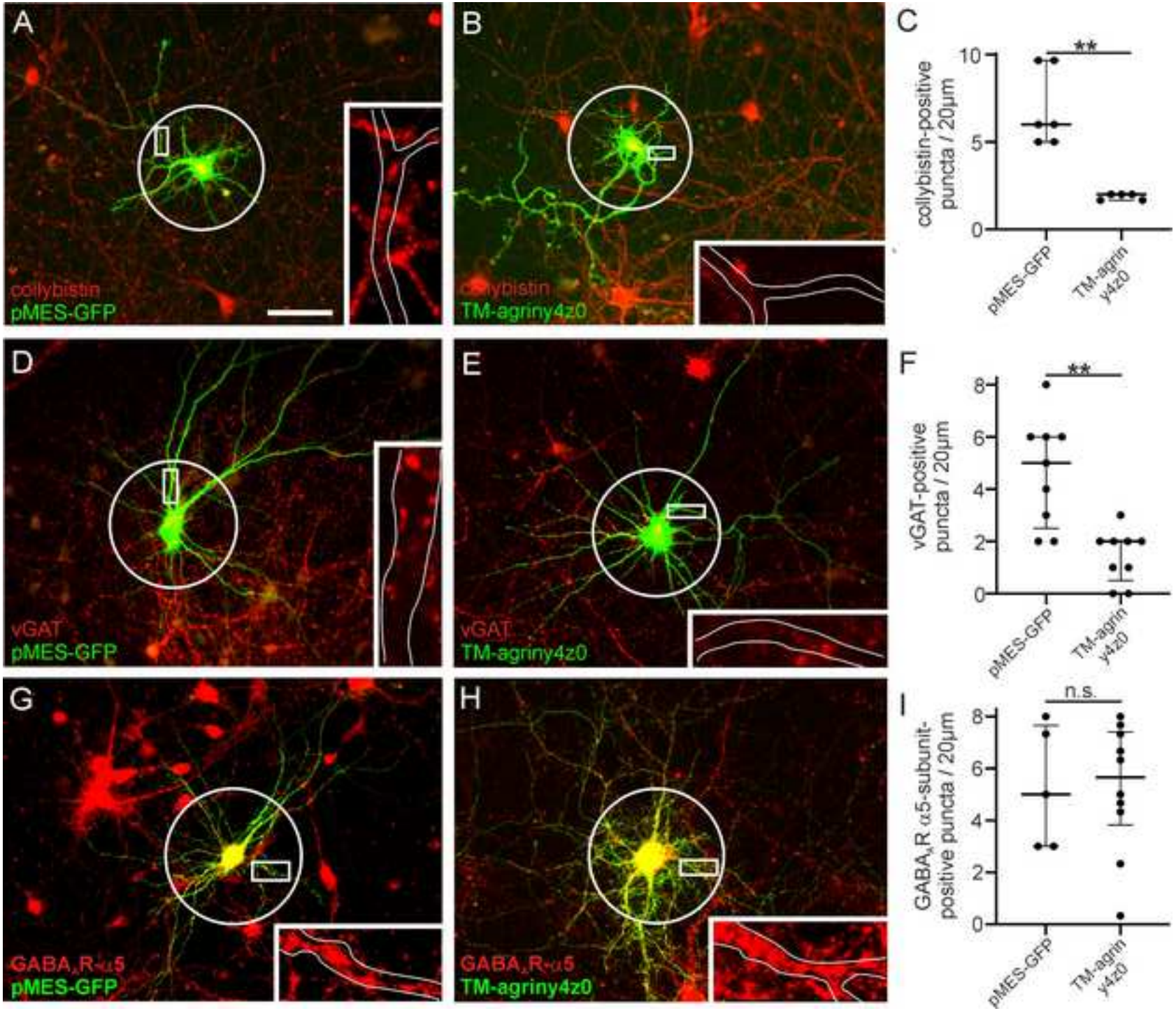

Figure 5

Click here to download high resolution image

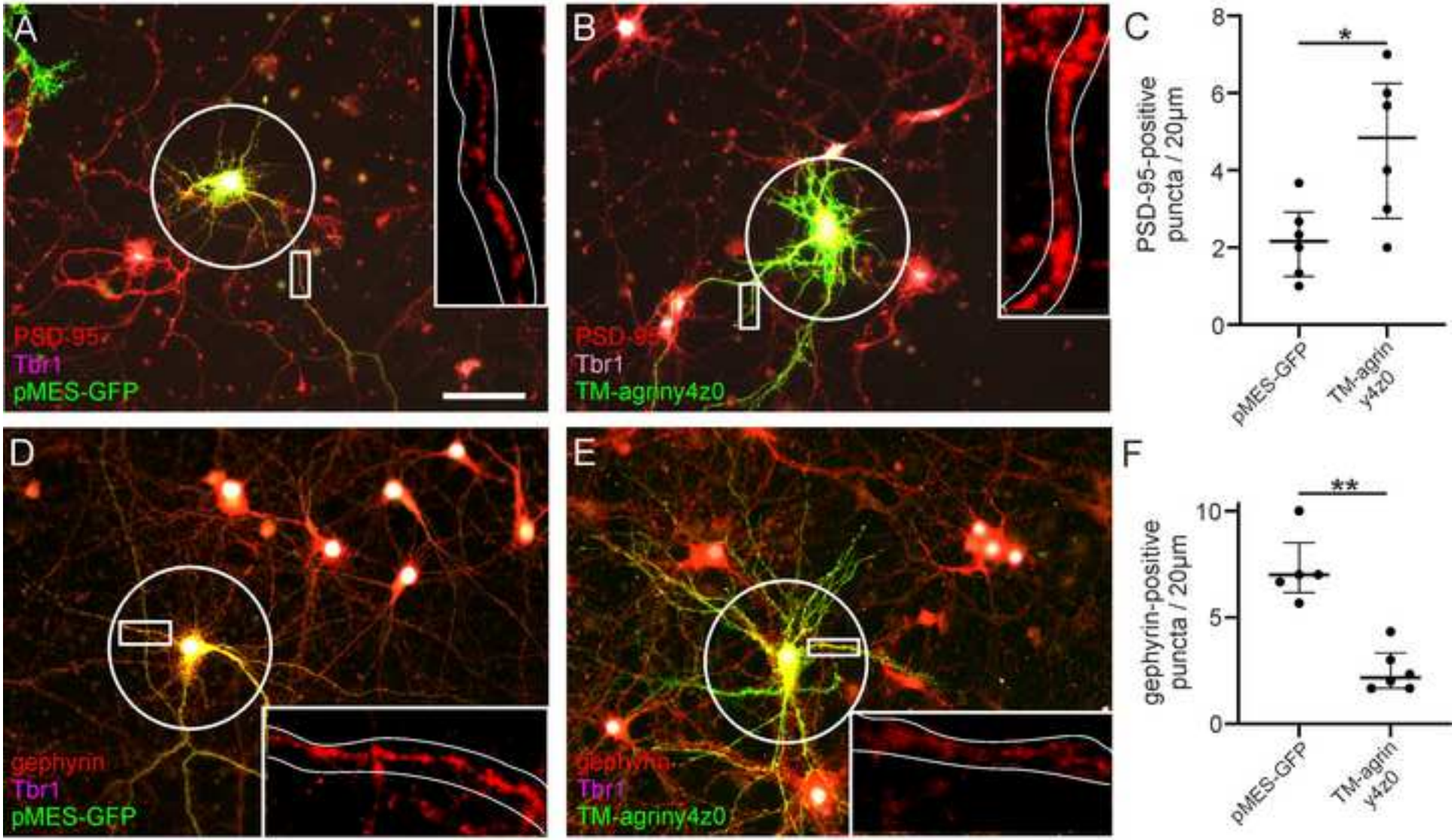

Figure 6

Click here to download high resolution image

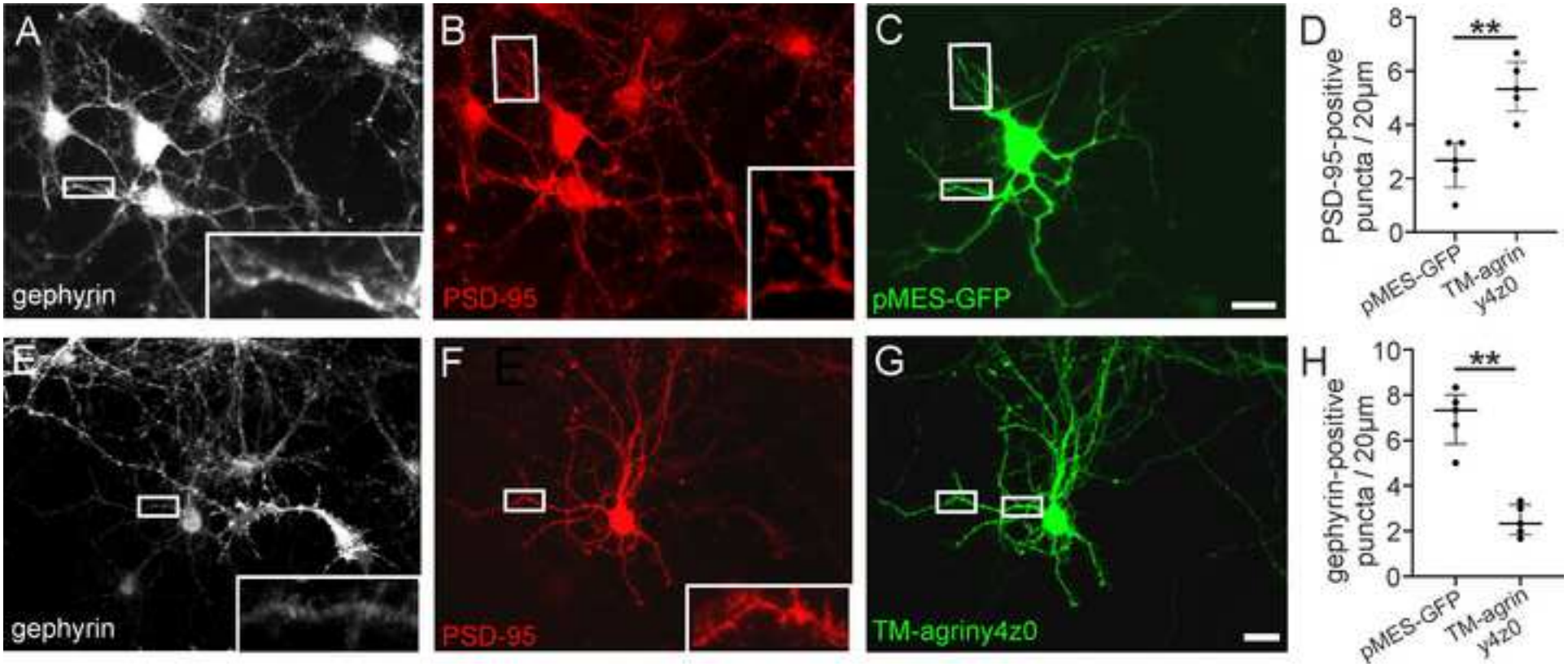

Figure 7

Click here to download high resolution image